

Cu-Ni Nanocatalysts in Mesoporous MCM-41 and TiO₂ to Produce Hydrogen for Fuel Cells via Steam Reforming Reactions

Richard Y. Abrokwa^{1, a}, Vishwanath G. Deshmane^{2, b}, Sri Lanka Owen^{3, c}
and Debasish Kuila^{3, d}

¹Department of Energy and Environmental Systems, North Carolina Agricultural and Technical State University (NCAT) Greensboro, NC 27411 USA

²Department of Chemical, Biological and Bioengineering (NCAT) Greensboro, NC 27411 USA

³Department of Chemistry (NCAT) Greensboro, NC 27411 USA

^aryabrokw@aggies.ncat.edu, ^bvishwa212003@gmail.com, ^cssowen@aggies.ncat.edu,
^ddkuila@ncat.edu

Keywords: one-pot hydrothermal synthesis; methanol conversion and H₂ selectivity; CO selectivity; Cu-Ni; mesoporous silica; titania bimetallic catalysts.

Abstract. We have synthesized mesoporous SiO₂ (MCM-41) and TiO₂ encapsulated bimetallic Cu-Ni nanocatalysts using an optimized one-pot hydrothermal procedure. The catalysts were characterized using N₂ adsorption-desorption isotherms (BET), X-ray diffraction (XRD), thermogravimetric and differential calorimetric analysis (TGA-DSC) and high-resolution transmission electron microscopy (HRTEM) techniques. Results show that bimetallic Cu-Ni/MCM-41 catalysts possessed significantly high surface area in the range of 634-1000 m²/g compared to Cu-Ni/TiO₂ which showed a surface area in the range 250-350 m²/g depending on the total metal loading (5-10 wt%). The small angle XRD studies confirmed a long range ordered structure in the Cu-Ni/MCM-41 catalysts. Wide angle XRD studies affirmed the presence of the catalytically active anatase phase in the crystalline Cu-Ni/TiO₂ bimetallic system. The results from HRTEM studies were consistent with the mesoporosity of both supports. These catalysts are tested for methanol conversion and H₂/CO selectivity via steam reforming of methanol (SRM) reactions in a down flow fixed bed reactor. Our investigations revealed a distinct contrast in the performance of both supports. While Cu is mainly responsible for the reforming activity in MCM-41, Ni bolstered the methanol conversion in TiO₂ supported catalysts. Bimetallic 3.33%Cu6.67%Ni/TiO₂ catalyst showed an impressive 99% H₂ selectivity at as low as 150 °C and a maximum conversion of 92% at 250 °C but 3.33%Cu6.67%Ni/MCM-41 catalyst did not show any H₂ selectivity at 150 °C and only ~12% conversion at 250 °C. The effect of each support and relative metal loadings on the activity and selectivity of the SRM reaction products at different temperatures is discussed.

Introduction

The quest to supplement non-replenishable fossil fuel energy with an array of renewable energy sources is the paramount goal of the 21st century to help mitigate the prevalent global energy shortages and environmental crisis. Recent strict Environmental Protection Agency (EPA) pollution by-laws and global energy shortages has incited active research and development in fuel cells. Hydrogen, the primary feedstock for proton exchange membrane fuel cells (PEMFC), is expected to play a critical role in the future of green energy economy. This is due to the fact that combustion of hydrogen produces zero carbonaceous greenhouse gases, thus reducing urban smog normally caused by emissions from gasoline and diesel engines. More significantly, it reduces overdependence on foreign oil, and H₂ has a low mass per unit energy and the same combustion efficiency as gasoline [1].

Steam reforming of alcohols (methanol, ethanol, glycerol) is one of the promising routes to produce H₂ to power fuel cells. For instance, methanol which is biodegradable possesses high H/C ratio and has no C–C bond which facilitates the reforming reaction at low temperatures (200–300 °C) with a low tendency for soot formation or catalyst coking. Also because it exists as liquid at

room temperature, on-board storage and refueling systems required is compatible with current commercial gasoline distribution infrastructure. However, the reaction yields CO as a by-product which readily poisons and incapacitates the platinum electrodes used in fuel cells. Thus, the design of the catalyst for the steam reforming reactions (SRRs) is critical in terms of reducing the CO formation. Various catalysts have been reported in the literature for the SRM reactions [2, 3, 4]. While copper (Cu) is active for steam reforming of methanol, it suffers from deactivation due to sintering after a long time on-stream and formation of CO as byproduct. Nickel (Ni) is also reported to be highly selective towards H₂ and when it is mixed with Cu, it can improve the CO₂ selectivity [5, 6].

The catalyst support plays a significant role in the activity and selectivity of the catalyst for steam reforming reactions [7-10]. Mesoporous material containing metal nanocatalysts is an exciting area of research because of its unique magnetic, optical, catalytic and electronic properties which is a product of the quantum-size synergistic effects between participating metal particles. These properties can be further adjusted by the addition of the second metal; because one metal has the tendency to regulate and modify the magnetic as well as the catalytic attributes of the other metal due to electronic and structural effects [11]. In this work, we report synthesis and characterization of high surface area MCM-41 and mesoporous TiO₂ encapsulated bimetallic Cu-Ni nanocatalysts and their reactivity studies in SRM reactions to produce hydrogen. We also seek to examine if any synergistic effects exist between Cu and Ni metals towards conversion and selectivity for the SRM gaseous products.

Experimental

Materials and Methods

Analytical grade reagents were used without further purification. Tetramethylorthosilicate, 99% (TMOS), Titanium (IV) isopropoxide (TIPR) and Ammonium Hydroxide, reagent ACS were obtained from Acros Organics, New Jersey, USA. Hexadecyltrimethyl-ammonium bromide minimum (CTAB) and Cu (II) Nitrate Hydrate, 98% ACS reagents were purchased from Sigma-Aldrich, Missouri, USA. Nickel Nitrate, Ethanol Anhydrous and ACS reagents were purchased from Fischer Scientific, New Jersey, USA. De-ionized water used at each stage was obtained from a Mill-Q Advantage A10 with Elix 5 system manufactured by Millipore Corporation (Bedford, MA, USA).

Catalyst Synthesis

For Cu-Ni/MCM-41, molar ratios of different components used were 1 TMOS: 0.13 CTAB: 130.6 H₂O: 20 Ethanol and specific amount of copper and nickel nitrate as per the required Cu and Ni loading [12]. In a typical synthesis of Cu-Ni/MCM-41, CTAB was dissolved in de-ionized water at 30 °C to get a colorless solution-A. Another solution designated B was prepared by dissolving required quantities of copper nitrate and nickel nitrate in ethanol. Solution B was gently poured into A and stirred for 30 minutes. To this solution, TMOS was added drop-wise and the solution was stirred for another 30 minutes. Ammonium hydroxide was then added to this solution drop-wise until the pH of the solution was 10 and stirred for another 3 h. The resulting material was aged in an oven at 65 °C for 18 h. The solid material was washed with deionized water until the pH of the filtrate was 7; it was filtered, followed by ethanol washing. The residue was first air dried for ~24 h and then dried in an oven at 110 °C for 24 h. Finally, the material was calcined at 550 °C for 16 h with a heating and cooling rate of 2 °C/min to remove CTAB completely.

For the synthesis of Cu-Ni/TiO₂ catalyst, TIPR was the limiting reagent and a molar ratio of 1 TIPR: 0.2 CTAB: 110.9 H₂O: 45.25 Ethanol was used. Precipitation with ammonium hydroxide was followed with aging for 24 hours at room temperature. The Cu-Ni/TiO₂ was then calcined at 450 °C (at 5 °C min⁻¹) for 6 h in static air to remove the organic template and to improve cross-linking of the inorganic polymer.

Catalyst Characterization

Brunauer-Emmett-Teller (BET) surface area, pore volume and pore size were determined using a Quantachrome NOVA 2200e instrument. Adsorption-desorption isotherms were generated by dosing nitrogen onto the material in a bath of liquid nitrogen at 77 K. The small and wide angle XRD diffractions were recorded using a D8 Discover X-ray diffractometer from Bruker (Bruker Optics, Inc., Billerica, MA). Thermogravimetric (TGA) and differential scanning calorimetry analyses (DSC) were carried out using a SDT Q600 V20.4 Build 14 system (TA Instruments, New Castle, DE, USA). The morphological properties of the catalysts were analyzed using Zeiss Libra 120 transmission electron microscope operated at an accelerating voltage of 120 kV.

Steam Reforming of Methanol (SRM)

Cu-Ni/MCM-41 catalyst was activated *ex-situ* in a tubular furnace using 4% hydrogen in argon at 550 °C for 5 h. Cu-Ni/TiO₂ was activated under similar conditions at 350 °C for 3 h. The activity tests for both catalysts were performed at atmospheric pressure in a continuous up down flow stainless steel fixed bed reactor (Tube ID: 6.22 mm). The activated catalyst was mixed with white quartz sand in a volume ratio of catalyst/sand 2:1. The mixture was then loaded into the reactor occluded with quartz wool at both ends. The catalyst was further activated *in-situ* at 350 °C for 1 h under 4% H₂ in argon environment just before the steam reforming reactions. A methanol/water feed molar ratio of 1:3 and flow rate of 2838 h⁻¹ GHSV at STP was maintained for all experiments. The temperature of the reactions was varied from 150 to 350 °C. The composition of the reaction products and collected condensate was analyzed using an Agilent 7890B GC equipped with TCD and FID detectors.

Results and Discussions

BET Analysis

Table 1 and Table 2 show the results of N₂ physisorption studies of Cu-Ni/MCM41 and Cu-Ni/TiO₂ catalysts, respectively. The surface area of the crystalline Cu-Ni/TiO₂ catalysts varied from 172 m²/g to 413 m²/g depending on the metal loading. Table 1 shows the textural properties of Cu-Ni/MCM41 catalysts ranging from 5 to 15 wt%. The amorphous Cu-Ni/MCM-41 catalysts showed a large surface area which decreased consistently with increasing metal loading (1000 m²/g to 634 m²/g). This trend could be due to the blocking of the mesopores by metal particles leading to an increase in the average pore size and a concomitant decrease in the catalytic surface area.

Table 1. Surface Area, Pore size and Pore volume of Cu-Ni-MCM41Catalysts

Metal Loading [wt%]		Surface Area [m ² /g]	Pore Size [nm]	Pore Volume [cm ³ /g]
Cu	Ni			
MCM-41 Only		1039.24	3.298	0.7450
5	10	635.08	3.656	0.6032
10	5	634.25	3.656	0.5958
3.33	6.67	807.64	3.775	0.7600
6.67	3.33	813.89	3.775	0.7166
1.67	3.33	1009.35	3.418	0.8468
3.33	1.67	977.33	3.537	0.7646

Table 2. Surface Area, Pore size and Pore volume of Cu-Ni-TiO₂ Catalysts

Metal [wt%]		Surface Area [m ² /g]	Pore Size [nm]	Pore Volume [cm ³ /g]
Cu	Ni			
TiO ₂ Only		137.219	4.33	0.1978
1.33	3.67	413.41	3.04	0.2534
3.67	1.33	350.34	3.30	0.2199
3.33	6.67	226.55	3.31	0.1621
6.67	3.33	172.83	3.32	0.1229

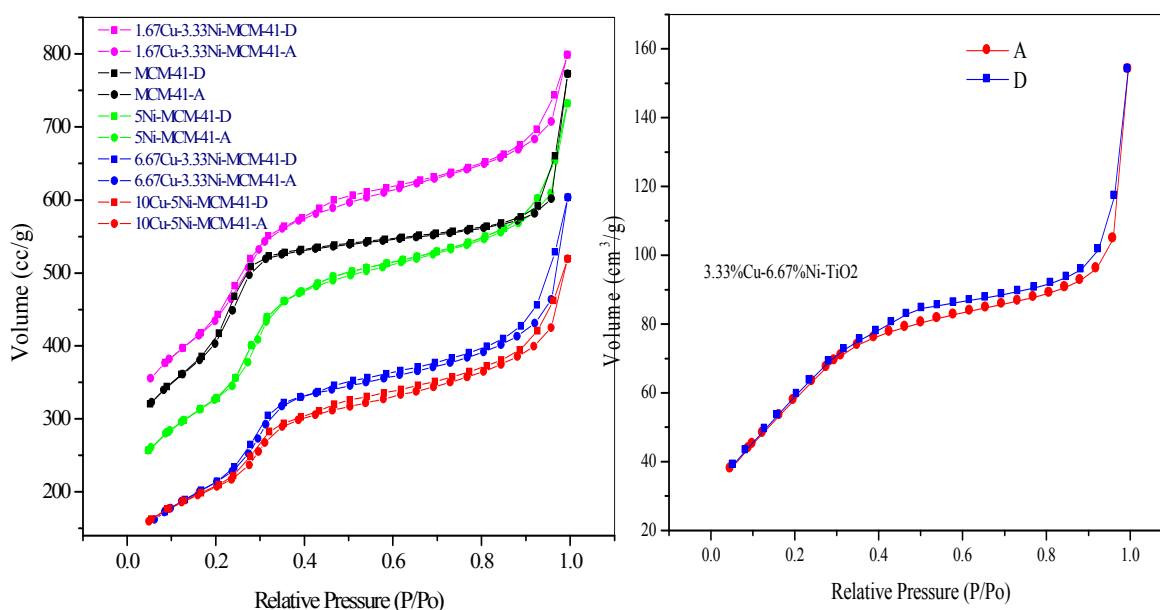


Fig. 1 N₂ Adsorption-Desorption Isotherms of (left) Cu-Ni/MCM-41 and (right) Cu-Ni-TiO₂ Catalysts

The isotherms of all the bimetallic systems in Fig. 1 show a typical type IV isotherm (according to the IUPAC nomenclature) indicative of mesoporous materials. In MCM-41 the steep rise at relative pressure ($P/P_0 = 0.21$ to 0.35) signifies the capillary condensation. The sharp gradient of this step is attributed to the narrow pore size distribution in the mesoporous structure. A sharp rise in N₂ adsorption associated with a hysteresis loop could be seen at relative pressure above 0.92 for the both catalysts. This is due to the intra-particle pore condensation of the N₂-adsorbate in both catalysts.

XRD Analysis of Catalysts

Fig. 2 shows SXRD of MCM-41 supported catalysts. The MCM-41 without metals showed the most intense peak (2theta range of 1.5° - 3°) indicative of a long range ordered mesoporous support. The intensity decreased only slightly at 5 wt% metal loading. However, at 15 wt% metal loading, a small shoulder peak could be observed, implying that some degree of ordered structure was still present at that high metal loading. No intense peaks were observed in the wide angle XRD of the Cu-Ni/MCM-41 catalysts. This could be due to the amorphous nature of the metal particles and also the preferential orientations of the metal crystallites in the support, leading to very little or no metal diffraction peaks.

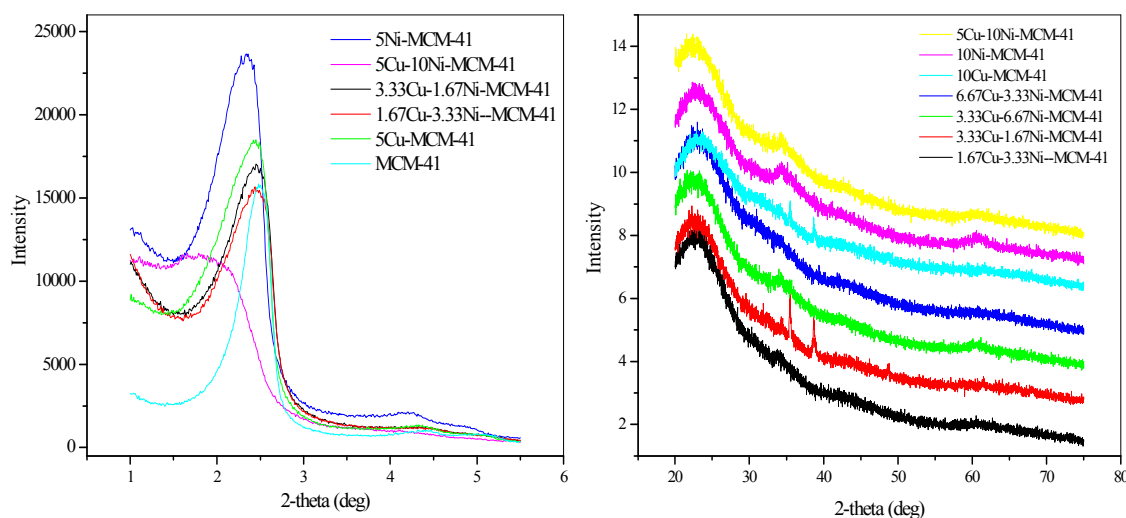


Fig. 2 Small angle (left) and wide angle (right) X-ray diffractograms of both mono and bimetallic Cu-Ni/MCM-41 catalysts

The wide angle X-ray diffraction pattern of 6.67%Cu3.33%Ni/TiO₂ is shown in Fig. 3. The diffraction peaks at about 25°, 38°, 48°, and 55° are characteristic of the anatase phase of titania. This elucidates the presence of pure anatase phase and absence of the rutile and brookite phases in the 6.67%Cu3.33%Ni/TiO₂ catalyst.

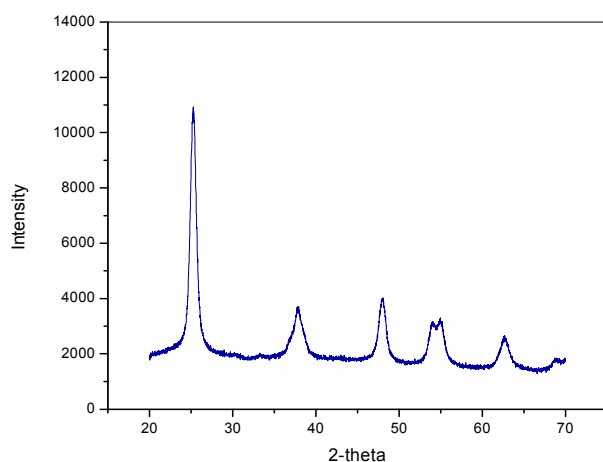


Fig. 3 Wide angle X-Ray diffraction spectrum of 6.67%Cu-3.33%Ni-TiO₂

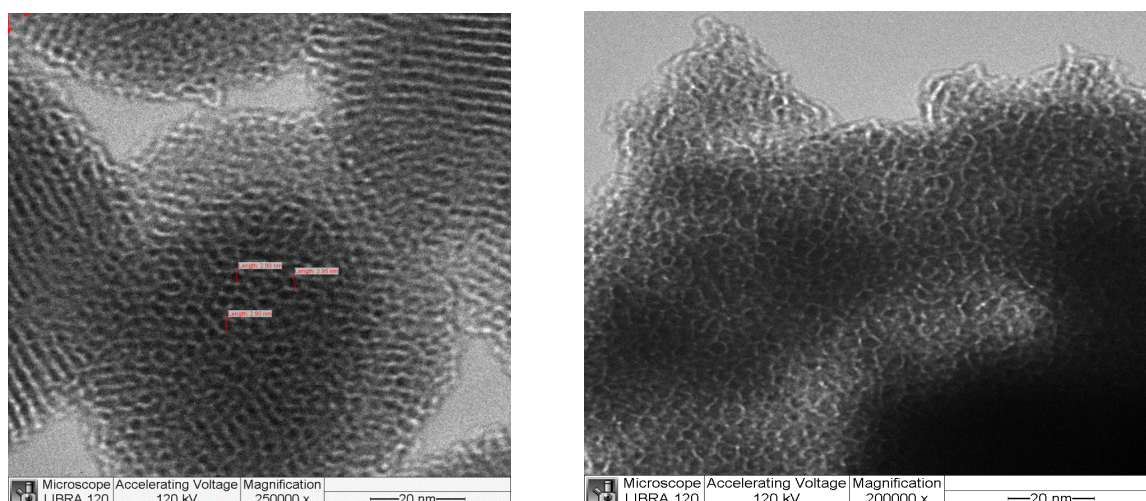


Fig. 4 TEM images of (left) MCM-41 and (right) TiO₂

The TEM micrographs of the MCM-41 and TiO₂ supported catalysts shown in Fig. 4 confirm the formation of ordered porous structure inferred from the small angle X-ray diffraction studies.

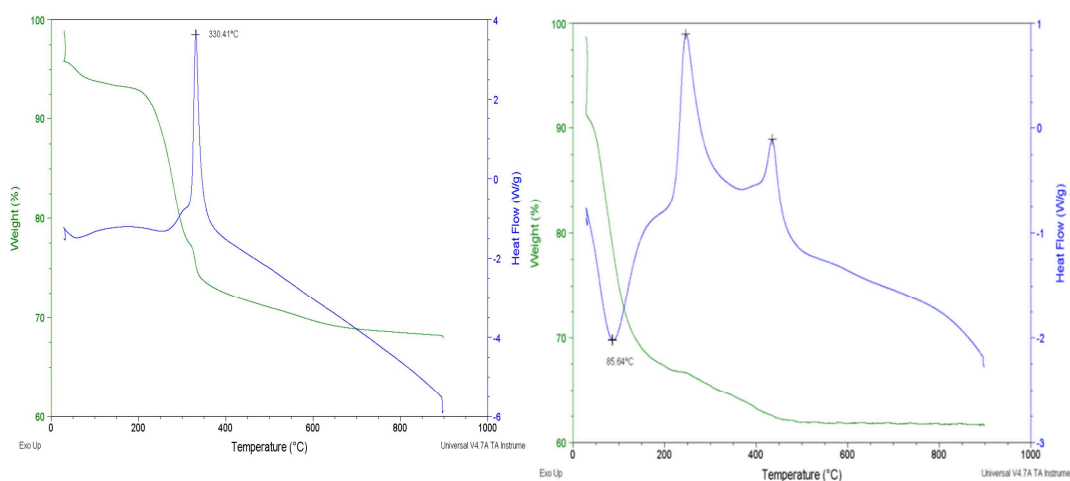


Fig. 5 TGA-DSC profiles for (left) MCM-41 (right) mesoporous TiO₂

Fig. 5 shows the TGA-DSC profiles of MCM-41 and mesoporous TiO₂ supports recorded in air environment. For both materials, the endothermic weight loss from 30 °C to 180 °C is attributed to the removal of water and other volatiles adsorbed on the surface of catalyst. Whereas the exothermic decomposition of the surfactant (CTAB) in the crystalline TiO₂ occurred at about 250 °C, for amorphous MCM-41 the removal temperature was 330 °C. In the thermogram of TiO₂, the second conspicuous exotherm observed around 450 °C-500 °C is attributed to the crystallization of the TiO₂ to the anatase phase.

Steam Reforming of Methanol Reactions with Catalysts

Methanol conversion and H₂/CO selectivities were calculated by using eq1-3.

$$\text{Conversion} : X_{\text{Methanol}} = \frac{\text{moles of CH}_3\text{OH converted}}{\text{moles of CH}_3\text{OH in feed}} \times 100\% \quad (1)$$

$$S_{\text{H}_2} = \frac{\text{moles of H}_2 \text{ produ} \quad \text{g}}{\text{moles of H}_2 \text{ produ} + 2 \times \text{g in product}} \times 100\% \quad (2)$$

$$S_{\text{CO}} = \frac{\text{produ} \quad \text{g}}{\text{moles of CO}_2 \text{ produ} + \text{produ} \quad \text{g} + 4 \text{ produ} \quad \text{g}} \times 100\% \quad (3)$$

Table 3 and Table 4 show the results of methanol steam reforming reactions on representative Cu-Ni/MCM-41 and Cu-Ni/TiO₂ catalysts, respectively.

Table 3. Methanol steam reforming with Cu-Ni/MCM41 Catalysts. MeOH/H₂O mole ratio: 1:3 GHSV: 2838 hr⁻¹ at STP

Catalyst	Temp. [°C]	Conversion [%]	Selectivity [%]			
			H ₂	CO	CO ₂	CH ₄
3.33%Cu6.67% Ni/MCM41	200	6.38	99.85	92.73	7.12	0.15
	250	12.08	100	94.48	5.52	0
	300	14.37	100	97.82	2.18	0
10%Cu-5%Ni/MCM-41	200	32.12	100	83.35	16.65	0
	250	37.04	100	92.21	7.79	0
	300	70.38	100	96.50	3.50	0
10Cu/MCM-41	200	53.91	100	4.2	95.8	0
	250	67.81	100	5.58	94.42	0
	300	69.94	100	16.36	83.64	0

All MCM-41 supported catalysts showed increasing methanol conversion as temperature increased from 200 °C to 300 °C, attributed to the endothermic nature of the methanol steam reforming process. When the Cu content was increased from 3.33 wt% to 10 wt%, methanol conversion increased almost 5-folds. This suggests that on MCM-41 support, Cu is mainly responsible for the reforming activity. SRM with 10%Cu-MCM-41 showed ~ 70% conversion at 300 °C, 100% H₂ selectivity and ~16% CO selectivity. However, upon addition of Ni to Cu catalyst, the CO selectivity increased significantly from ~16% to ~96% with about 70% methanol conversion at 300 °C. This suggests that, Ni addition could be favoring the reverse water gas-shift reaction or decreasing the water-gas shift reaction activity via negative synergistic effect producing significantly large amount of CO.

Table 4. Methanol steam reforming with Cu-Ni/TiO₂ Catalysts. MeOH/H₂O mole ratio: 1:3 GHSV: 2838 hr⁻¹ at STP

Catalyst	Temp. [°C]	Conversion [%]	Selectivity [%]			
			H ₂	CO	CO ₂	CH ₄
6.67%Cu3.33%Ni-TiO ₂	150	-	99.38	30.42	68.66	0.92
	200	67.58	99.77	38.14	61.55	0.31
	250	79.66	99.76	50.95	48.76	0.29
3.33%Cu6.67%Ni-TiO ₂	150	-	-	-	-	-
	200	82.69	91.61	60.44	25.53	14.03
	250	91.18	89.73	66.12	22.16	11.73

One striking difference between MCM-41 and TiO₂ supported catalysts was that the SRM activity of Cu-Ni/TiO₂ is observed at as low as 150 °C in contrast to Cu-Ni/MCM-41 which showed negligible activity at that temperature. Furthermore, at 250 °C, 3.33Cu6.67Ni/MCM41 showed a considerably lower conversion of ~12% compared to ~92% for the 3.33Cu-6.67Ni-TiO₂. TiO₂ supported bimetallic catalysts showed a significantly lower CO selectivity and insignificant amount of CH₄ compared to the Cu-Ni/MCM-41 catalysts. This clearly shows that TiO₂ is a better support for Cu-Ni bimetallic catalyst relative to SiO₂. It was also observed that as Ni content was increased from 3.33% to 6.67%, methane selectivity increased from ~1% to about 14%, indicating the well known methanation activity of Ni catalysts. On the other hand, when the Cu content is increased from 3.33% to 6.67%, the CO selectivity decreased from about 66% to 50% at 250 °C, indicating the water-gas shift activity of Cu catalysts.

Conclusions

We have synthesized high surface area Cu-Ni/MCM-41 and Cu-Ni/TiO₂ bimetallic catalysts by an optimized one-pot hydrothermal procedure. The N₂ adsorption-desorption studies confirmed the mesoporous nature of both catalysts. However, small angle XRD analyses showed that only the Cu-Ni/MCM-41 catalyst possessed a long range ordered mesoporous structure even at metal loading as high as 15wt%. Wide angle XRD confirmed the catalytically active anatase phase of the Cu-Ni/TiO₂ catalysts. It was observed that an addition of Ni to Cu-MCM-41 catalyst significantly increased CO selectivity indicating negative influence of Ni on SRM selectivity. Compared to MCM-41 catalysts, TiO₂-supported catalysts showed higher SRM activity and significantly lower CO selectivity. However, it also showed certain activity for methanation reaction which increased with increase in Ni content. Thus, it can be concluded that the specific metal-support interactions are unique and dictate the relative conversion and selectivity for each product-gas component of methanol steam reforming.

Acknowledgements

We acknowledge NSF support for this work (CREST, Grant No.HRD-124215). The authors would like to thank Mr. James King (Chemistry Department) for his support in the experimental work of this project. We also acknowledge Dr. Sergey Yarmolenko (Center for Advanced Materials), Dr. Ilias (Chemical Engineering Dept. NCAT) and the Joint School of Nanoscience and Nanoengineering for hosting our catalyst characterization studies.

References

- [1] Shriver & Atkins, Inorganic Chemistry, fourth ed., W. H. Freeman and Company, New York, 2006, 170,702.
- [2] S. Yong, C. Ooi, et al, Review of methanol reforming-Cu-based catalysts, surface reaction mechanisms, and reaction schemes, *Int. J. Hydrogen Energy*, (2013), 9541–9552
- [3] J. Abolfazl, M.A.A. Seyed, B. Bahamin, A.J. Moradian, Enhancement in thermal and hydrothermal stabilities of novel mesoporous MCM, *J. Porous Mater* (2012), 19, 979- 988.
- [4] P. Lo'pez, G. Mondrago-Galicia, M.E. Espinosa-Pesqueira, D. Mendoza-Ana. Hydrogen production from oxidative steam reforming of methanol: Effect of the Cu and Ni impregnation on ZrO₂ and their molecular simulation studies *Int. J. Hydrogen Energy*, (2012), 37, 9018–9027.
- [5] S. Sá, H. Silva, L. Brandão, J.M. Sousa, A. Mendes, Catalysts for methanol steam reforming- A review, *App. Catalysis B: Environmental* (2010), 99, 43-57.
- [6] M. Khzouz, J. Wood, B. Pollet, W. Bujalski, Characterization and activity test of Commercial Ni/Al₂O₃, Cu/ZnO/Al₂O₃ and prepared Ni–Cu/Al₂O₃ catalysts for hydrogen production from methane and methanol fuels, *Int. J. Hydrogen Energy*, (2013), 38, 1664-1675.
- [7] A. Bshish, Z. Yaakob, B. Narayanan, B.; Ramakrishnan, R.; Ebshish, A. Steam-reforming of ethanol for hydrogen production. *Chem. Papers*. (2011), 65, 251-266.
- [8] Y. Yang, J. Ma, et al, Production of hydrogen by steam reforming of ethanol over a Ni/ZnO catalyst. *Int. J. Hydrogen Energy*, (2006), 31, 877-882.
- [9] G. Gabriella, R. Paola, A. L. Mattia, Cobalt-based nanoparticles as catalysts for low temperature hydrogen production by ethanol steam reforming. *Int. J. Hydrogen Energy*, (2013), 38, 82-91.
- [10] V. Nichelea, M. Signoretto, F. Menegazzo, Glycerol steam reforming for hydrogen production : Design of Ni supported catalysts, *App. Catalysis B: Environmental*, (2012), 225 - 232.
- [11] Kosaraju, K., Rahman, A., Duncan, M., Tatineni, B., Basova, Y., Deshmane, V., Abrokwah, R., Hosseinezhad, S., King, J., and Ilias, S. *Future Energy, Environment, and Materials*, (2014), 88,337
- [12] B. Tatineni, S. Islam, Y. Basova, A. Rahman, et al, Development of Mesoporous Silica Encapsulated Pd-Ni Nanocatalyst for hydrogen production, *ACS Symposium series* (2011), 177-190.